Pulsed magnetic field generation system for laser-plasma research

A G Luchinin, V A Malyshev, E A Kopelovich, K F Burdonov, M E Gushchin, M V Morozkin, M D Proyavin, R M Rozental, A A Soloviev, M V Starodubtsev, et al.

Pulsed magnetic field generation system for laser-plasma research

A.G.Luchinin, V.A.Malyshev, E.A.Kopelovich, K.F.Burdonov, M.E. Gushchin, M.V.Morozkin, M.D.Proyavin, R.M.Rozental, A.A.Soloviev, M.V.Starodubtsev, A.P.Fokin, J.Fuchs, and M.Yu.Glyavin

Institute of Applied Physics RAS (IAP RAS), Nizhny Novgorod, 603950 Russia
pmd@appl.sci-nnov.ru

Abstract

An up to 15 T pulsed magnetic field generator in a volume of a few cubic centimeters has been developed for experiments with magnetized laser plasma. The magnetic field is created by a pair of coils placed in a sealed reservoir with liquid nitrogen, installed in a vacuum chamber with a laser target. The bearing body provides the mechanical strength of the system both in the case of co-directional and oppositely connected coils. The configuration of the housing allows laser radiation to be introduced into the working area between the coils in a wide range of directions and focusing angles, place targets away from the symmetry axis of the magnetic system, and irradiate several targets simultaneously.

Keywords: plasma, laser, pulsed magnetic field, intense fields, co-directional and oppositely connected coils

1. Introduction

Pulsed magnetic fields are widely used in various devices and systems, including laser-plasma research. Interest in these works is largely stimulated by the search for new schemes for laser-plasma generation of charged particle beams and problems of controlling their characteristics, including the collimation of charged particle beams [1–3]. Work in the field of high energy density physics is another important application of magnetic fields with induction of more than 10 T in laser-plasma research. Here, the prospect of creating a magnetized laser plasma opens up wide experimental opportunities for studying the entire spectrum of problems, ranging from laboratory modeling of astrophysical phenomena (including the study of the formation mechanisms of astrophysical jets [4, 5], accretion flows [6] and the conditions for the development of MHD [7] and other types of instabilities [8] that arise during the interaction of plasma flows with a magnetic field) to the development of new directions in controlled thermonuclear fusion related to using external magnetic fields to magnetize to magnetize the electrons, which then thermalize with the ion population thereby increasing ion temperature [9–11], reduce losses due to limiting the electron thermal conductivity [12], and suppress hydrodynamic instabilities [13, 14], as well as to implement other methods of increasing the efficiency of heating a thermonuclear target [15].

In this paper, we describe a pulsed magnetic system created at the IAP RAS for research in high energy density physics and laboratory astrophysics at the PEARL laser-plasma facility [16]. Section 2 defines the requirements for the magnetic system. Section 3 contains a description of its design and the results of measurements of the parameters of the magnetic system. Section 4 formulates the results of the work and provides brief data on experiments using the created magnetic system.

2. Justification of the parameters of the magnetic system for a high-energy laser-plasma experiment

This paper presents an experimental platform for studying the processes of interaction of high-speed laser plasma flows with an external magnetic field. Specifically, we are going to study the expansion of high-velocity laser plasma flows into both uniform and non-uniform magnetic fields and the excitation of instabilities in such a system and other similar subjects that are of great interest for laboratory astrophysics.

The experimental platform is based on a magnetic system that generates magnetic fields with induction $B_0 > 10$ T on centimeter scales. The platform provides the possibility of forming a laser plasma flow inside the magnetic system and its diagnostics. In the experimental approach of interest to us, the initial gas-dynamic pressure of the laser plasma significantly exceeds the pressure of the background magnetic field. As a result the laser plasma cloud expands freely into the magnetic field at the initial stage. Due to the high conductivity (typical magnetic Reynolds numbers in such experiments: $R_m \sim 10^2 – 10^3$, see,

for example, [17]), the magnetic field at this stage can be considered frozen into the plasma. As a result, the magnetic field strength inside the expanding plasma volume rapidly decreases, and a diamagnetic plasma cavity is formed, which is in contact with the external magnetic field. The characteristic size of the cavity, determined by the equality of the plasma pressure and the magnetic pressure, can be estimated as $R_b \sim (3E_0/B_0^2)^{1/3}$ [18, 19], where E_0 is the energy of the plasma cloud, the characteristic values of which under the conditions of laser-plasma experiments usually lie in in the range of 1–100 J [4-7]. Obviously, in the experiments on the interaction of a laser plasma with an external magnetic field, the characteristic scale L of the latter should be several times larger than R_b to make it possible to study not only the formation of a diamagnetic cavity but also the dynamics of further interaction of the plasma with the magnetic field and background medium.

A significant number of experimental studies of the interaction of plasma clouds with an external magnetic field are performed at $B_0 \sim 0.01 - 0.1$ T [20-22]. In this case, the characteristic dimensions of the plasma cloud lie in the range $R_b \sim 10 - 1000$ cm and the characteristic plasma densities turn out to be of the order of 10^{14} cm^{-3}. The main methods for studying plasma dynamics under these conditions are high-speed photography and probe techniques.

When creating our experimental platform, we used a different approach based on the use of magnetic fields with an induction of the order of 10 T. Under these conditions, the characteristic size R_b turns out to be of the order of several millimeters, and the characteristic electron density reach values of the order of 10^{17} - 10^{19} cm^{-3}. Such concentration values give us a number of advantages from a diagnostic point of view. In particular, we can use optical diagnostic methods, first of all, femtosecond laser interferometry, making it possible to obtain practically instantaneous "snapshots" of the two-dimensional distribution of the concentration in the plasma flow with a high spatial-temporal resolution.

This simple reasoning leads to the following requirements for the parameters of the magnetic system: the magnetic field is no less than 10 T, the dimensions in all directions are no less than 1 cm, and the pulse duration of the magnetic field is much more than 10 ns (the latter is determined by the characteristic time of plasma expansion to the size R_b, see, for example, [7]). In addition, the magnetic system should provide access of high-power and diagnostic laser radiation to the target in the widest possible range of angles and directions.

An example of an experimental scheme for studying the interaction of a laser-produced plasma with an external magnetic field is shown in Fig. 1. A laser pulse (wavelength ~ 527 nm, pulse duration ~ 1 ns, and energy ~ 1–100 J) irradiates the surface of a solid target (Teflon). The target is located inside the coils that create a locally uniform magnetic field. In this geometry, the plasma flow propagates mainly in the direction perpendicular to the target surface. The characteristic velocity of the plasma flow in such experiments is 100–1000 km/s.

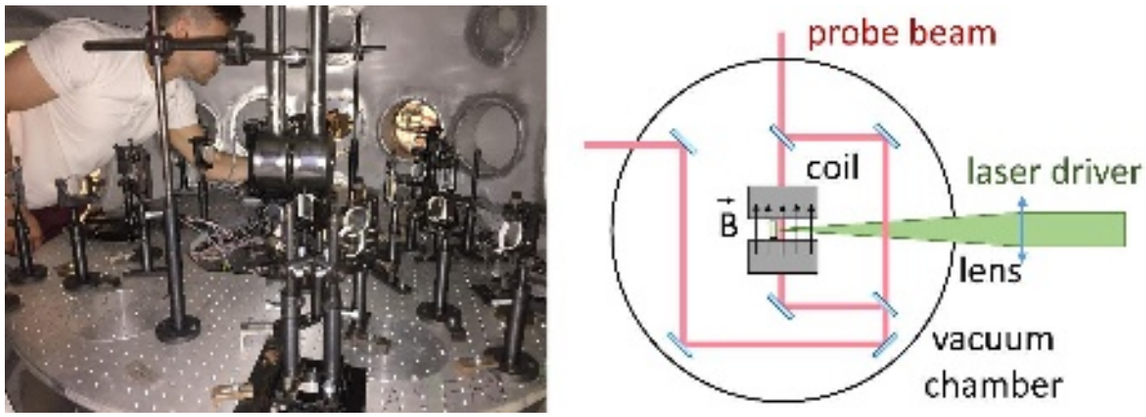

Fig. 1. A photograph of the experimental chamber (left) and the experiment scheme (right) for studying the interaction of the laser plasma flow with an external magnetic field. Horizontal arrows indicate the magnetic field direction.

The current laser-plasma experiments with magnetic fields of 10 T or more use miniature disposable coils, which, as a rule, are destroyed by the flow of a pulsed current and as a result of exposure to high-power laser radiation [23, 24]. The need to replace the coils after each shot of the laser setup creates inconveniences during the experiment. The variant of stationary coils protected from laser radiation by a metal shell and effectively cooled between shots of the laser setup seems more promising. Since laser-plasma experiments are performed in high vacuum chambers, and a typical pulse repetition rate of laser radiation is one pulse per several tens of minutes, it is expedient to use a cryostat filled with liquid nitrogen to cool the coils. As a result, the simplest stationary magnetic system can consist of a pair of coils separated by more than 1 cm and fixed in a sealed housing with double walls, between which liquid nitrogen is poured. In this case, along with the mechanical strength and vacuum tightness, the housing design should provide the following capabilities:

- setting up a target attached to the positioning system;
- input and output of a diagnostic laser beam with a diameter of at least 1 cm in two mutually perpendicular directions;
- the ability to input high-power laser radiation in a wide range of angles with respect to the direction of the magnetic field.

The last point imposes one more restriction on the design of the magnetic system. Indeed, to create a laser-produced plasma by substance ablation from the surface of a solid target, the intensity of nanosecond laser radiation on the target surface should be of the order of 10^{11}–10^{15} W/cm^2. Typical parameters of a nanosecond laser beam that will be used in experiments are as follows: duration 1 ns (Gaussian), energy less than 100 J, and diameter 10 cm. The wavefront quality of the nanosecond channel at the PEARL facility allows focusing down to the size of approximately two diffraction limits. An F/10 focusing was employed in the experiments, which allowed spot sizes starting from 40 μm (at level $\frac{1}{e^2}$) and more. Thus, the

structural elements of the magnetic system should not interfere with such focusing of laser radiation into the central region of the magnetic system. Simple estimates show that for the given parameters, intensities up to $8 \cdot 10^{15}$ W/cm^2 may be reached. For optical diagnostics of plasma (see Fig. 1), a laser beam with a duration of 50 fs (Gaussian) at a wavelength of 910 nm is used. The diagnostic beam diameter is 2.5 cm, energy is 10 mJ. The limitations of the optical diagnostics field of view caused by the magnetic system design are as follows: round-shaped (2.1 cm in diameter) along the axis of the magnetic system and oval-shaped (1.1 cm × 2 cm) in the perpendicular direction. The dynamics of plasma expansion is studied in a series of shots by changing the delay between the femtosecond diagnostic and plasma-generating nanosecond laser pulses (the delay line is not shown in Fig. 1).

The requirements for the magnetic field uniformity in the region where the laser plasma interacts with the magnetic field are not very high, since, in any case, in the course of experiments, the magnetic field is strongly disturbed by the invading plasma flow, and the process of magnetic field penetration into the plasma is accompanied by the development of instabilities at the boundary between plasma and magnetic field. When designing the magnetic system described below, we restricted ourselves to the requirements for the magnetic field uniformity of the order of $\frac{\Delta B_0}{B_0} \leq 10\%$ in the gap between coils.

The studies of the processes of interaction of a laser-produced plasma of high energy density with a magnetic field are not limited to the case of a locally uniform distribution of the magnetic field. A number of problems on laboratory modeling of space plasma phenomena require the creation of highly non-uniform magnetic fields near the target, including the points with a zero magnetic field. Such problems include modeling of plasma processes during magnetic reconnection [25] and various aspects of the dynamics of accretion disks [26]. In particular, setting up model experiments on the entrainment of a magnetic field by a rotating plasma, which were proposed in [26], requires the creation of a magnetic configuration of the "cusp" type. Modeling of the laser plasma transfer processes between the regions with zero field and the regions in which electrons and ions are completely magnetized involves the creation of magnetic field gradients of a level of several tesla per millimeter near the target. A zero-point cusp magnetic field configuration that meets this requirement can be created by the same pair of coils when they are connected in opposite directions.

3. Design of the magnetic system and test results

The main elements of the magnetic system are shown in Fig. 2. The design is based on the principles detailed in [27]. Namely, 1) the solenoid was wound with a rectangular-section copper wire followed by making it monolithic with epoxy compound, 2) liquid nitrogen was used for cooling, 3) the energy storage recharging (recovery) circuit was rejected in order to ensure the minimum voltage between the grounded housing and the adjacent turns of the coils. Particular attention was paid to the configuration of holes in the

housing that provide a plasma channel with a passage diameter of 21.5 mm in the center of the magnetic system, which opens near the edges at an angle of 11 deg to the channel axis. In the perpendicular plane, four conical channels, 12 mm wide and having aperture angles of 78 deg, were made for observation and diagnostics. The magnetic system mounting flange is located on the semispherical cover of the vacuum chamber. An insignificant displacement of the flange, and accordingly the axis of the magnetic system, with respect to the fixed axis of the laser beam propagation during evacuation, can be counterbalanced by the bellows assembly, which provides positioning of the magnetic system axis within 20 mm.

The magnetic system is composed of two multi-turn coils wound on a stainless-steel housing and is designed to operate in a single pulse mode. For winding, we used enameled copper wire of rectangular section. The characteristics of the coils are given in Table 1. The pulse repetition rate is determined by the Joule loss in the coils and the time required for cooling. To reduce the ohmic resistance of the wires (about 7 times compared to room temperature) and additional thermal stabilization of the initial state, the coils are immersed in a bath with liquid nitrogen. According to the results of theoretical calculations, the repetition rate for the magnetic system is approximately one pulse every two minutes. The appearance of the assembled magnetic system is shown in Fig. 2 (c). The placement of the magnetic system in the target chamber of the PEARL stand is shown in the left photo in Fig. 1: the magnetic system is attached to the upper cover of the target chamber through a vacuum seal. With the help of a bellows, clearly visible in Fig. 2 (c), the position of the magnetic system in the center of the target chamber is fine-tuned.

Table 1. Parameters of the coils.

Cross-sectional dimensions of copper wire	3 x 1 mm
Number of turns in each layer	5
Number of layers	18
Cross-sectional dimensions of the whole coil	17.5 x 30 mm
Coordinates of the centers of the cross-section of each coil	R = 27.5 mm, Z = ± 18.75 mm

For the magnetic system, we developed a power supply that provides the formation of a given magnetic field in the operating volume of the solenoid with inductance *Ls* and active resistance *Rs* when a capacitive energy storage (CES) with capacitance *C* is discharged to it via a thyristor switch *VS* [28]. The block diagram of the power supply and the oscillogram of the current pulse are shown in Fig. 3. The main parameters of the power supply are summarized in Table 2 and the parameters of the coils of the magnetic system in Table 3.

The simplest estimate of the inductance of the single coil can be made according to the Perry formula [29], which in the International System of Units has the form

$$L = \frac{\mu_0 R^2 N^2}{0.2317R + 0.44b + 0.39c} \quad (1)$$

where μ_0 is the vacuum permeability, R is the radius of the center of the coil, b is the axial width, c is the radial width. For our coil R = 27.5 mm, b = 17.5 mm, and c = 30 mm (see Table 1) Perry's formula gives an inductance of 300 μH, which is quite consistent with a measured inductance of 350 μH (see Table 3). Direct calculation of the inductance using COMSOL Multiphysics® [30] gives a value of 320 μH, which also agrees with the experimental results.

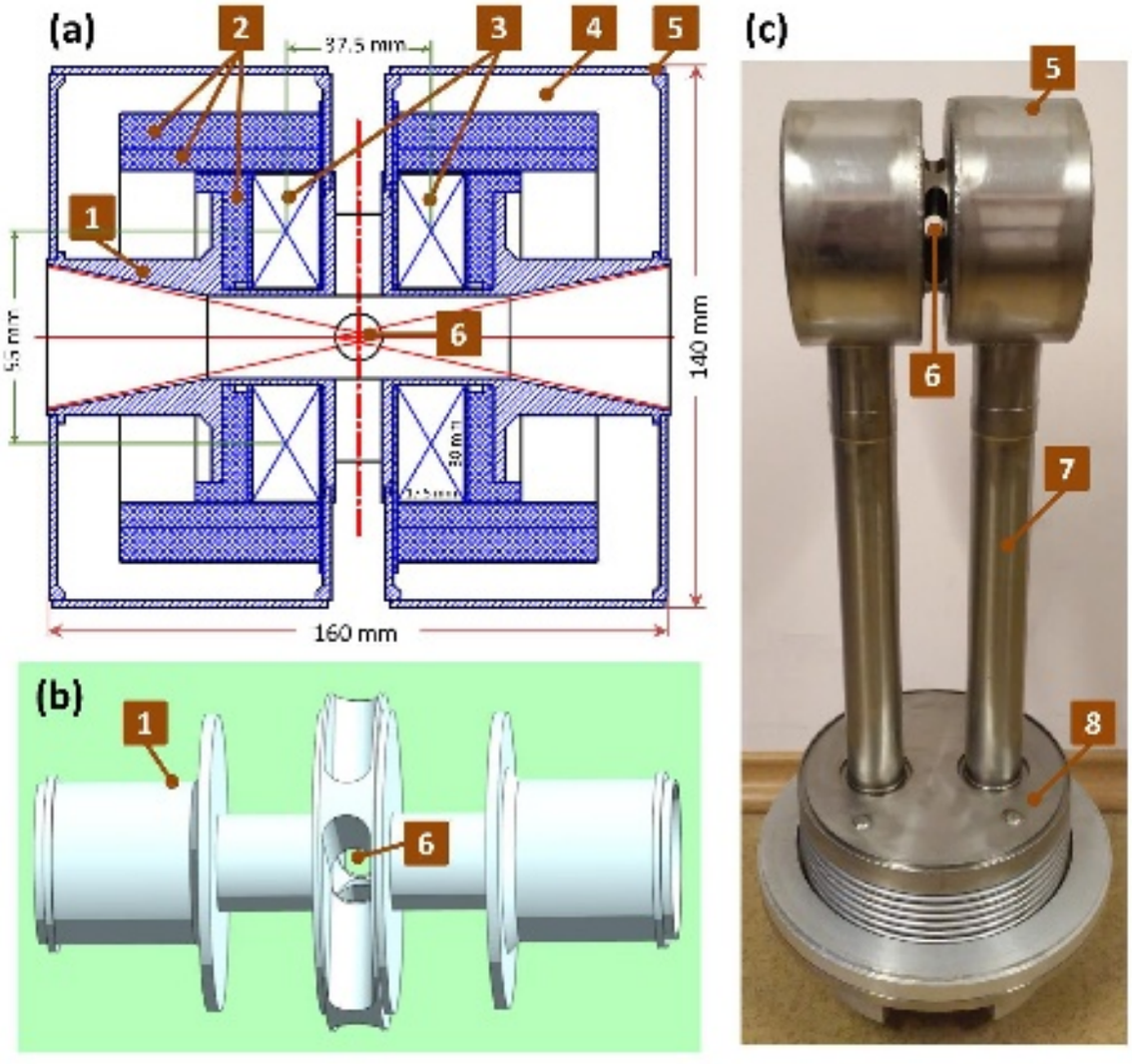

Fig. 2. A schematic sectional view of the magnetic system (a), a 3D model of the metal load-bearing frame (b), and the appearance of the manufactured magnetic system (c). The numbers indicate the following: 1 - metal load-bearing frame, 2 - composite elements of the load-bearing frame, 3 - windings, 4 - nitrogen chamber, 5 - external shield, 6 - conical holes for laser radiation input and plasma flow output, 7 - channels for liquid nitrogen supply and placement of current

leads, and 8 - vacuum-tight bellows docking unit.

Table 2. Main parameters of the power supply of the magnetic system.

Charge voltage control range	0.2 - 3.9 kV
Maximum admissible amplitude of the current pulse	8 kA
Charge voltage instability in the range 0.2 -1.5 kV in the range 1.5 - 3.9 kV	 < 1% < 0.2%
Capacitance of the storage capacitor *C* (see fig. 3a)	3300 μF
Resistance of R_{cr} (see fig. 3a)	0.1 Ohm

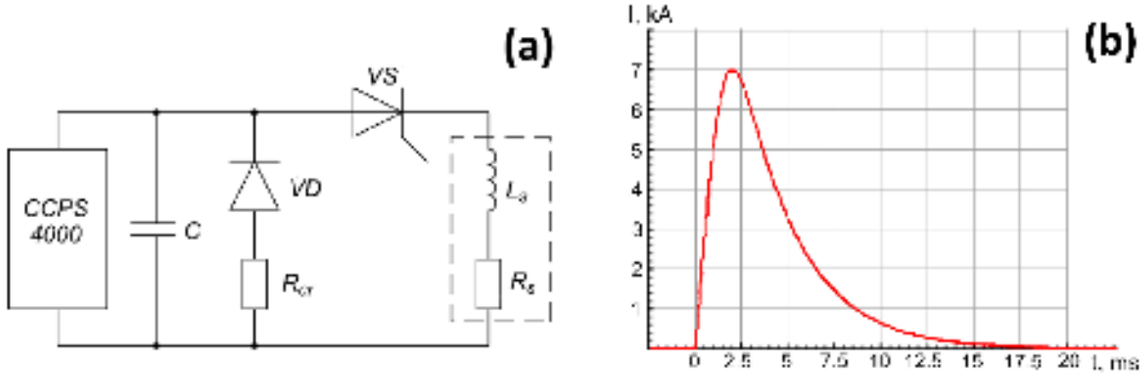

Fig. 3. Block diagram of the power supply of the magnetic system (a), and current pulse oscillogram (b).

Table 3. Measured parameters of the magnetic system coils.

Inductance of a single coil	350 μH
Inductance of the system with the coils connected in series and co-directed	760 μH
Inductance of the system with the coils connected in series and counter-directed	650 μH
Ohmic resistance of a single coil at room temperature	100 mOhm

The design of the magnetic system makes it possible (by switching external connections) to use oppositely connected coils or employ only one coil to significantly extend the range of possible experiments. In particular, this will permit one to study the interaction of plasma flows with non-uniform magnetic fields and the processes of separation of plasma flows from the diverging magnetic field lines.

Figure 4 shows the results of experimental measurements of the longitudinal profile of the magnetic field on the axis of the system with in-series and oppositely connected coils, which were performed with a direct current of 5 A using a Hall sensor (field meter model

TESLA RLCG Bridge-Voltmeter BM 559). Measurements of the field in the section z = 0 and r about 7 mm showed a decrease in the magnetic field by about 4% relative to the values at r = 0. All the results meet the requirements for laser experiments, in particular, the field uniformity length in the longitudinal and radial directions is twice the characteristic size of the studied plasma (~10 mm) and agree with theoretical calculations.

Since we are not able to measure the magnetic field directly during the passage of a kiloampere current through the coils, we obtain the magnitude of the magnetic field on the axis indirectly, through the measurement of the coil current:

$$B(I,z) = B_{ref}(z) \cdot \frac{I}{I_{ref}} \tag{2}$$

where $B(z)$ is the magnetic field on the axis of the system in the z coordinate, $B_{ref}(z)$ is the reference magnetic field, which we obtain from the experimental data shown in Figure 4, I_{ref} is the current at which the magnetic field values $B_{ref}(z)$ were measured, and I is the coil current.

We assume that the ratio (2) is preserved in operating regimes, since the weakening of the magnetic field of the coils by the stainless steel power frame is small. To determine the magnitude of the shielding of the magnetic field by the force frame of the coil, we made a simple estimate based on the well-known formula for the weakening of the magnetic field by a thin conducting cylinder (see, for example, [31]):

$$\frac{H_i}{H_0} = \frac{1}{\sqrt{1 + \left(\frac{R \cdot d}{\delta^2}\right)^2}} \tag{3}$$

where H_i/H_0 is the ratio of the shielded magnetic field (inside the conducting cylinder) to the unperturbed solenoid field, $\delta = 1/\sqrt{\pi f \mu_0 \sigma}$ is the skin depth, f is the effective frequency of the magnetic field oscillations, σ is the conductivity of stainless steel, μ_0 is vacuum permeability, R is the inner radius of the cylinder and d is the wall thickness of the cylinder.

The pulse rise time is about 1.8 ms, so the effective frequency is about 140 Hz. The conductivity of AISI 321 stainless steel is about 13800 S/m at room temperature. We took the parameters of the cylinder according to the dimensions of the inner cylinder of the load-bearing frame: R = 10.75 mm, d = 1.5 mm. For these parameters, the weakening of the magnetic field $\Delta_H = 1 - H_i/H_0$ was approximately 0.01%. Numerical calculations in COMSOL, which fully consider all the elements of the frame and casing of the coils, temperature drift, etc, give a field weakening Δ_H of a few tenths of a percent.

Additional confirmation of this method of indirectly determining the magnetic field values are experiments with pulsed gyrotrons [32, 33], in which a high magnetic field (tens of Tesla) was created by solenoids made according to a technology similar to that described in this article. In these studies, the solenoid constant (the ratio of the field in the center of the solenoid to the current flowing through the winding) was also measured at a small direct current, and the total field was then calculated as proportional to the supplied current. In

experiments with gyrotrons, the field inside the coil can be estimated with high accuracy from the microwave radiation frequency ω under cyclotron resonance conditions: $\omega \approx \omega_c = {eB}/{mc\gamma}$. In these studies, the calculated fields coincided with the values of the fields determined from the frequency of the gyrotron radiation.

The maximum magnetic field produced by the device in co-directed coils mode is 15 T, which is confirmed experimentally (indirectly, by current, in accordance with the (2)). The limiting factor for co-directed coils was the power supply, and for oppositely connected coils – mechanical properties of the stainless-steel frame. In the maximum current regime, the system experiences significant mechanical loads, therefore, in the absence of an urgent need, the work was carried out at a current of 90% of the maximum, which corresponds to a magnetic field of 13.5 T.

Obviously, the system experiences the greatest mechanical loads when the coils are connected in opposition. To prevent mechanical destruction, it was decided to abandon the welded connection of the parts of the winding unit, and now the latter is made by mechanical (turning and milling) processing from a single workpiece. The mechanical loads and deformations were calculated using the COMSOL Multiphysics®. The mechanical load was analyzed for a pulsed current, but the following approximation was used: the force acting on the coils was calculated in the approximation of stationary coils, and then, based on this force, the mechanical load and the value of the mechanical displacement of the system elements were calculated. The calculation results for a 5 kA current with oppositely connected coils are shown in Fig. 5. The maximum displacement of the coil elements does not exceed 0.1 mm, and the maximum von Mises stress is 100 MPa, while the ultimate strength of the AISI 321 steel used for the manufacture of the coil frame is about 200 MPa at room temperature and only increases with cooling [34].

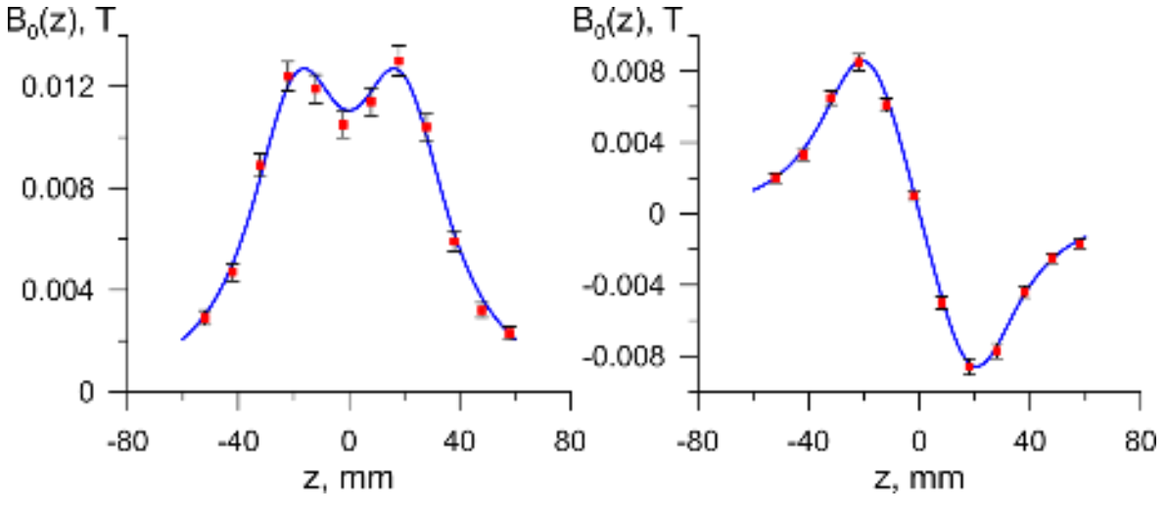

Fig. 4. Distribution of the magnetic field along the system axis in the modeling mode with a 5 A current: (a) co-directional connection of coils and (b) oppositely directed connection of coils (solid lines and dots show the calculation results and the measured values, respectively).

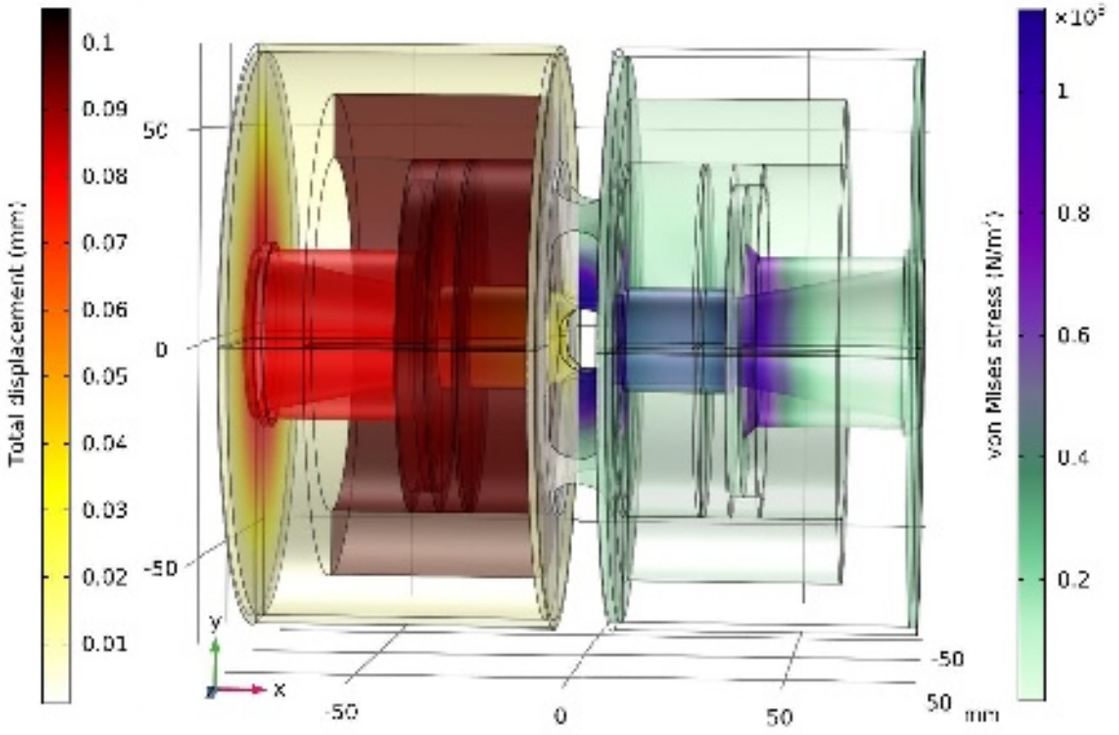

Fig. 5. Results of modeling of magnetic loads. The maximum displacement of the coil elements is shown on the left of the symmetry plane. The stress of the winding unit for a differently directed connection of solenoids with a 5 kA current is shown on the right.

4. Conclusions

A magnetic system has been created and successfully tested, which makes it possible to repeatedly generate pulses of a magnetic field with an intensity of up to 15 T. A key feature of the system is the possibility of both co-directional and oppositely directed connection of a pair of coils, which ensures a variety of magnetic field configurations.

At the moment, the operating time of the magnetic system is more than 1000 pulses, without any change in physical and technical parameters.

Using the described magnetic system, a number of successful experiments, described in, e.g., [35,36], were performed with the PEARL facility. An example of interferometric measurements of laser plasma expanding across a 13,5 T uniform ambient magnetic field is represented in Fig.6. The performed experiments are devoted, in particular, to laboratory modeling of astrophysical processes, as well as the processes of interaction of high-speed flows of hot dense laser plasma with external magnetic fields for modeling the magnetohydrodynamic processes developing in the vicinity of compact stars. Physical processes in the boundary layer between the moving plasma and the magnetic field were examined. This is a key factor for creating physical models of the inner edge of accretion disks, accretion columns, astrophysical jets, etc.

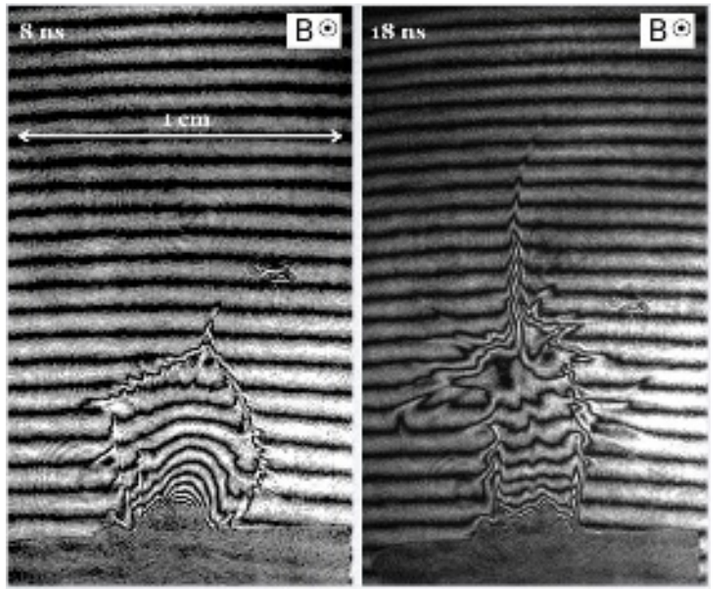

Fig. 6. Examples of interferometric measurements of laser plasma expansion across a uniform magnetic field (13.5 T, 90% of maximum field). Target: Teflon. Laser parameters: 527 nm, 1 ns, 20 J. Laser spot size: 350 μm.

Acknowledgements

This work was supported by the Russian State Assignment Program, IAP RAS project 0030-2021-0001, 0030-2021-0015, 0030-2021-0027.

Data Availability

The data that support the findings of this study are available from the corresponding author upon reasonable request.

References

1. R. Kodama, K. A. Tanaka, Y. Sentoku, T. Matsushita, K. Takahashi, H. Fujita, Y. Kitagawa, Y. Kato, T. Yamanaka, and K. Mima. Long-Scale Jet Formation with Specularly Reflected Light in Ultraintense Laser-Plasma Interactions // Phys. Rev. Lett. 84, 674 (2000).
2. S. Bolaños, J. Béard, G. Revet, S. N. Chen, S. Pikuz, E. Filippov, M. Safronova, M. Cerchez, O. Willi, M. Starodubtsev, et al. Highly-collimated, high-charge and broadband MeV electron beams produced by magnetizing solids irradiated by high-intensity lasers // Matter and Radiation at Extremes 4, 044401 (2019).
3. Hui Chen, G. Fiksel, D. Barnak, P.-Y. Chang, R. F. Heeter, A. Link, and D. D. Meyerhofer, "Magnetic collimation of relativistic positrons and electrons from high intensity laser–matter interactions", Physics of Plasmas 21, 040703 (2014) https://doi.org/10.1063/1.4873711
4. B. Albertazzi, A. Ciardi, M. Nakatsutsumi, T. Vinci, J. Béard, R. Bonito, J. Billette, M. Borghesi, Z. Burkley, S. N. Chen, et al. Laboratory formation of a scaled protostellar

jet by coaligned poloidal magnetic field // Science, 17 Oct 2014, Vol. 346, Issue 6207, pp. 325-328.

5. B. Albertazzi, J. Béard, A. Ciardi, et al., "Production of large volume, strongly magnetized laser-produced plasmas by use of pulsed external magnetic fields", Review of Scientific Instruments 84, 043505 (2013) https://doi.org/10.1063/1.4795551
6. E.P. Kurbatov, D.V. Bisikalo, M.V. Starodubtsev, A. Ciardi, J. Fuchs, A.A. Solov'ev, K.F. Burdonov, G. Revet, S. Chen. Comparison of dimensionless parameters in astrophysical MHD systems and in laboratory experiments. Astronomy Reports, V. 62, P. 483 (2018) doi: 10.1134/S1063772918080061
7. B. Khiar, G. Revet, A. Ciardi, K. Burdonov, E. Filippov, J. Beard, M. Cerchez, S.N. Chen, T. Gangolf, S.S. Makarov, et al. Laser-produced magnetic-Rayleigh-Taylor unstable plasma slabs in a 20 T magnetic field. Phys. Rev. Lett., V. 123, P. 205001 (2019) doi: 10.1103/PhysRevLett.123.205001
8. D.P. Higginson, Ph. Korneev, C. Ruyer, R. Riquier, Q. Moreno, J. Béard, S. N. Chen, A. Grassi, M. Grech, L. Gremillet, et al. Laboratory investigation of particle acceleration and magnetic field compression in collisionless colliding fast plasma flows // Communications Physics, 2019, V. 2, Art. no. 60.
9. P. Y. Chang, G. Fiksel, M. Hohenberger, J. P. Knauer, R. Betti, F. J. Marshall, D. D. Meyerhofer, F. H. Séguin, and R. D. Petrasso. Fusion Yield Enhancement in Magnetized Laser-Driven Implosions // Phys. Rev. Lett. 107, 035006, 15 July 2011.
10. J. R. Davies, D. H. Barnak, R. Betti, E. M. Campbell, P.-Y. Chang, A. B. Sefkow, K. J. Peterson, D. B. Sinars, and M. R. Weis, "Laser-driven magnetized liner inertial fusion", Physics of Plasmas 24, 062701 (2017) https://doi.org/10.1063/1.4984779
11. E. C. Hansen, J. R. Davies, D. H. Barnak, R. Betti, E. M. Campbell, V. Yu. Glebov, J. P. Knauer, L. S. Leal, J. L. Peebles, A. B. Sefkow, and K. M. Woo, "Neutron yield enhancement and suppression by magnetization in laser-driven cylindrical implosions", Physics of Plasmas 27, 062703 (2020) https://doi.org/10.1063/1.5144447
12. D. H. Froula, J. S. Ross, B. B. Pollock, P. Davis, A. N. James, L. Divol, M. J. Edwards, A. A. Offenberger, D. Price, R. P. J. Town, et al. Quenching of the Nonlocal Electron Heat Transport by Large External Magnetic Fields in a Laser-Produced Plasma Measured with Imaging Thomson Scattering // Phys. Rev. Lett. 98, 135001, 29 March 2007.
13. L.J. Perkins, B. G. Logan, G. B. Zimmerman, and C. J. Werner. Two-dimensional simulations of thermonuclear burn in ignition-scale inertial confinement fusion targets under compressed axial magnetic fields // Physics of Plasmas 20, 072708 (2013)
14. L.J. Perkins, D. D.-M Ho, B. G. Logan, G. B. Zimmerman, M. A. Rhodes, D. J. Strozzi, D. T. Blackfield, and S. A. Hawkins. The potential of imposed magnetic fields for enhancing ignition probability and fusion energy yield in indirect-drive inertial confinement fusion // Physics of Plasmas 24, 062708 (2017).

15. S. Sakata et al. Magnetized fast isochoric laser heating for efficient creation of ultra-high-energy-density states // Nature Communications, volume 9, Article number: 3937 (2018).
16. https://ipfran.ru/science/laser-physics-and-nonlinear-optics/generation-of-extreme-laser-fields/PEARL-laser-complex
17. D.P. Higginson, G. Revet, B. Khiar, J. Beard, M. Blecher, M. Borghesi, K. Burdonov, S.N. Chen, E. Filippov, D. Khaghani, et al. Detailed characterization of laser-produced astrophysically-relevant jets formed via a poloidal magnetic nozzle. High Energy Density Physics, V. 23, P. 48 (2017) doi: 10.1016/j.hedp.2017.02.003
18. Yu.P. Raizer. The deceleration and energy conversions of a plasma expanding in a vacuum in the presence of a magnetic field J. Appl. Mech. Tech. Phys., No. 6, P. 19 (1963, in Russian);
19. D Winske, J.D. Huba, C. Niemann, A. Le. Recalling and updating research on diamagnetic cavities: Experiments, theory, simulations. Front. Astron. Space Sci., V. 5, P. 51 (2019) doi: 10.3389/fspas.2018.00051
20. Yu.P. Zakharov. Collisionless laboratory astrophysics with lasers. IEEE Trans. Plasma Sci., V. 31, P. 1243 (2003) doi: 10.1109/TPS.2003.820957
21. A.S. Bondarenko, D.B. Schaeffer, E.T. Everson, S.E. Clark, B.R. Lee, C.G. Constantin, S. Vincena, B. Van Compernolle, S.K.P. Tripathi, D. Winske, et al. Laboratory study of collisionless coupling between explosive debris plasma and magnetized ambient plasma. Phys. Plasmas, V. 24, P. 082110 (2017) doi: 10.1063/1.4995480
22. M.E. Gushchin, S.V. Korobkov, V.A. Terekhin, A.V. Strikovskiy, V.I. Gundorin, I.Yu. Zudin, N.A. Aidakina, A.S. Nikolenko. Laboratory simulation of the dynamics of a dense plasma cloud expanding in a magnetized background plasma on a Krot large-scale device. JETP Letters, V. 108, P. 391 (2018) doi: 10.1134/S0021364018180054
23. O.V. Gotchev, P.Y. Chang, J.P. Knauer, D.D. Meyerhofer, O. Polomarov, J. Frenje, C.K. Li, M.J.-E. Manuel, R.D. Petrasso, J.R. Rygg, et al. Laser-driven magnetic-flux compression in high-energy-density plasmas. Phys. Rev. Lett., V. 103, P. 215004 (2009) doi: 10.1103/PhysRevLett.103.215004
24. G. Fiksel, A. Agliata, D. Barnak, G. Brent, P.-Y. Chang, L. Folnsbee, G. Gates, D. Hasset, D. Lonobile, J. Magoon, et al. Note: Experimental platform for magnetized high-energy-density plasma studies at the Omega laser facility. Rev. Sci. Instrum., V. 86, P. 016105 (2015) doi: 10.1063/1.4905625
25. R.A. Treumann, W. Baumjohann. Collisionless magnetic reconnection in space plasmas. Frontiers in Physics, doi: 10.3389/fphy.2013.00031 (2013)
26. D.D. Ryutov. Using intense lasers to simulate aspects of accretion discs and outflows in astrophysics. Astrophys. Space Sci., V. 336, P. 21 (2011) doi: 10.1007/s10509-010-

0558-9

27. M.Glyavin and A.Luchinin. A terahertz gyrotron with pulsed magnetic field // Radiophysics and Quantum Electronics, 2007, 50, 10-11, 755-761 doi: 10.1007/s11141-007-0066-0
28. M. Glyavin et al. A pulse magnetic field generator for terahertz gyrodevices // Instruments and Experimental Techniques 54(1):77-80, 2011
29. J. Perry, A formula for calculating approximately the self-induction of a coil // The London, Edinburgh, and Dublin Philosophical Magazine and Journal of Science, 30:184, 223-227, DOI: 10.1080/14786449008620016
30. www.comsol.com
31. S. Fahy, C. Kittel, and S. G. Louie, "Electromagnetic screening by metals," American Journal of Physics, vol. 56, no. 11, p. 989, Jul. 1998, doi: 10.1119/1.15353.
32. M. Yu. Glyavin, A. G. Luchinin, and G. Yu. Golubiatnikov, "Generation of 1.5-kW, 1-THz Coherent Radiation from a Gyrotron with a Pulsed Magnetic Field," Physical Review Letters, vol. 100, no. 1, p. 15101, 2008, doi: 10.1103/PhysRevLett.100.015101.
33. M. Yu. Glyavin et al., "A 670 GHz gyrotron with record power and efficiency," Applied Physics Letters, vol. 101, no. 15, p. 153503, 2012, doi: 10.1063/1.4757290.
34. McHenry H.I. (1983) The Properties of Austenitic Stainless Steel at Cryogenic Temperatures. In: Reed R.P., Horiuchi T. (eds) Austenitic Steels at Low Temperatures. Springer, Boston, MA
35. K. Burdonov et al., "Inferring possible magnetic field strength of accreting inflows in EXor-type objects from scaled laboratory experiments," Astronomy & Astrophysics, vol. 648, p. A81, Apr. 2021, doi: 10.1051/0004-6361/202040036.
36. A. A. Soloviev et al., "Experimental Study of the Interaction of a Laser Plasma Flow with a Transverse Magnetic Field," Radiophysics and Quantum Electronics 2021, vol. 63, no. 11, pp. 1–11, Oct. 2021, doi: 10.1007/S11141-021-10101-Y.

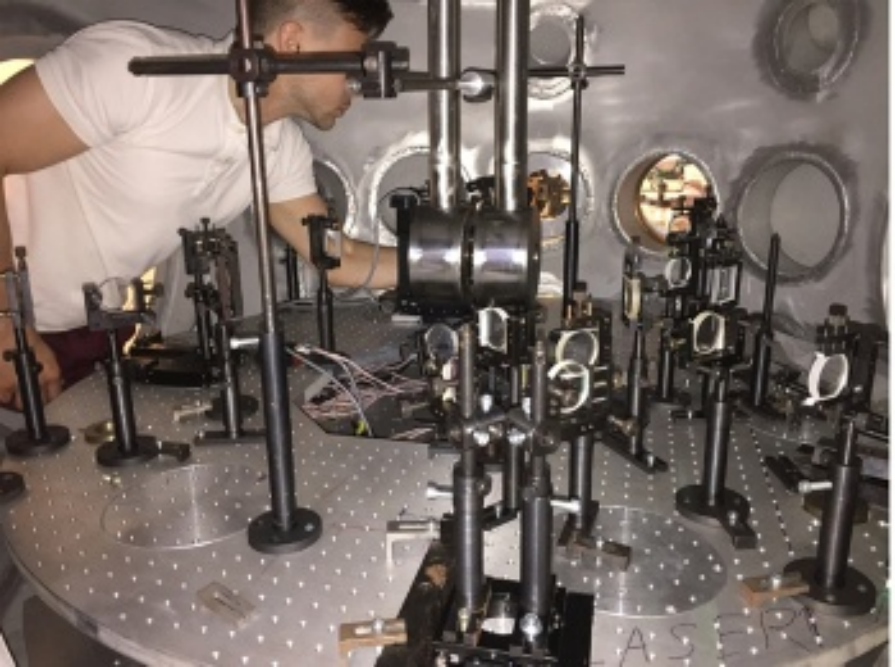

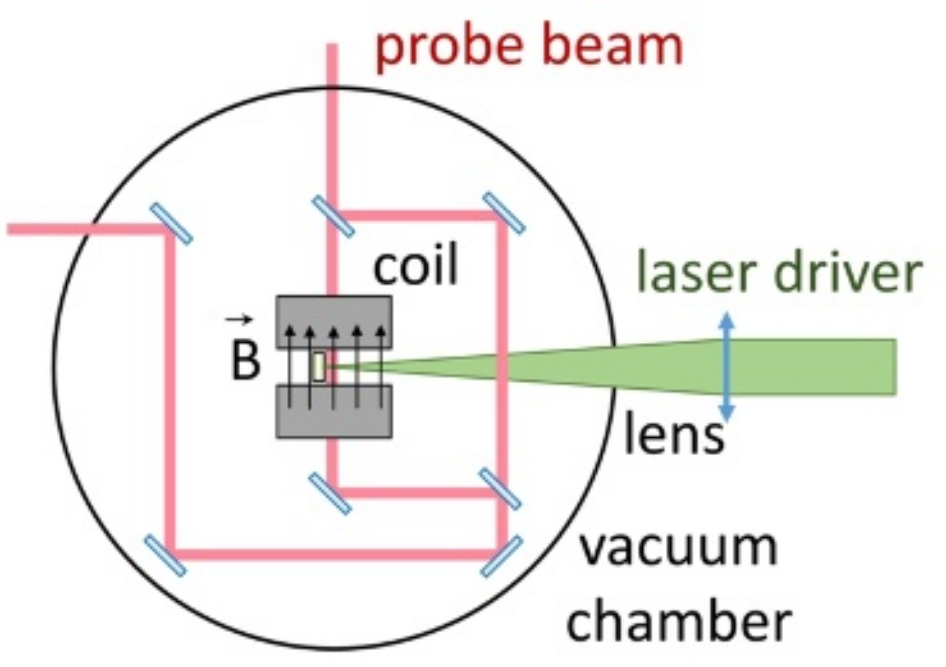
probe beam
coil
laser driver
B
lens
vacuum
chamber

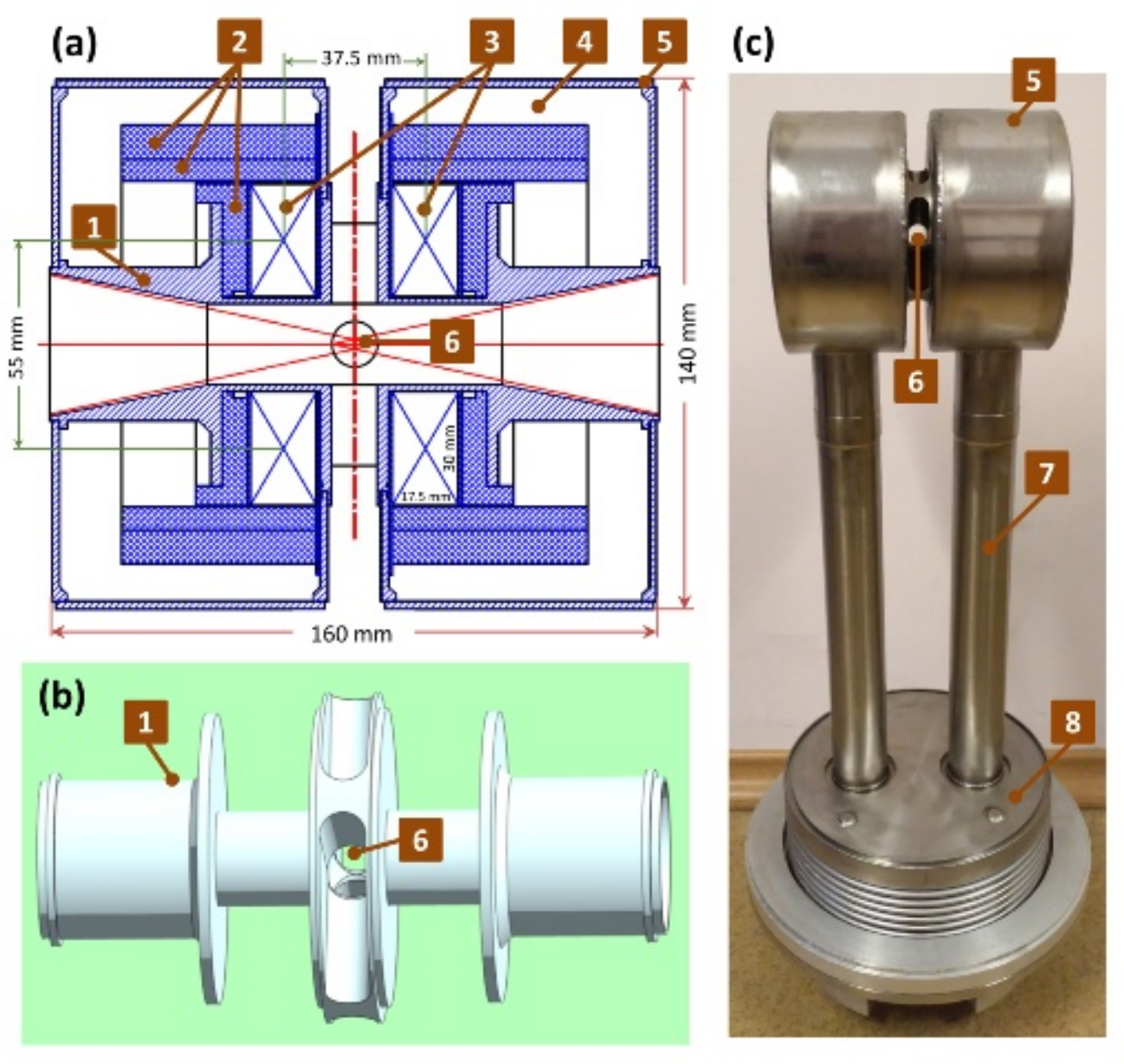
(a)
2
37.5 mm
3
4
5
1
6
55 mm
140 mm
30 mm
17.5 mm
160 mm
(b)
1
6
(c)
5
6
7
8

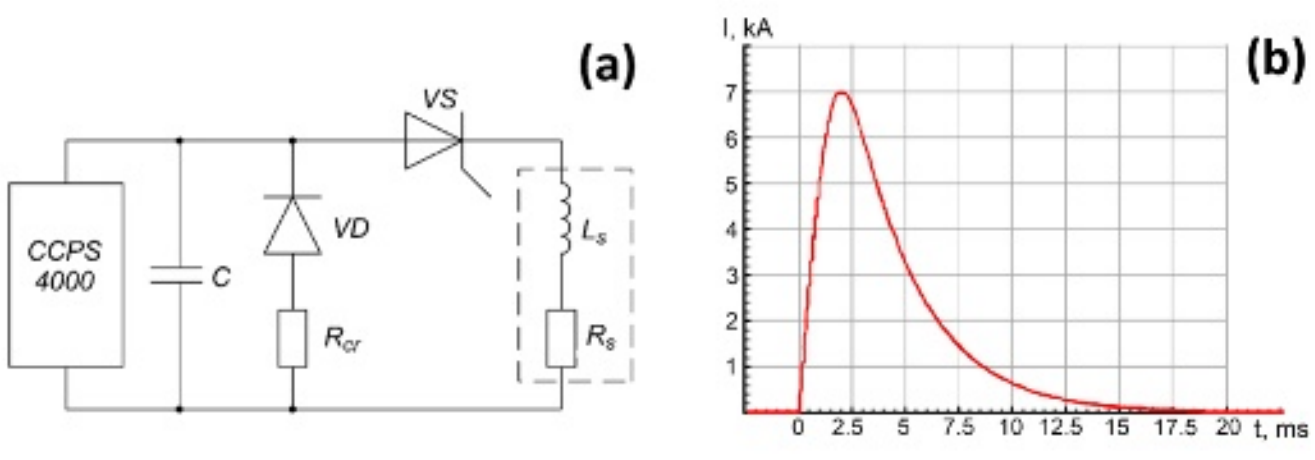
(a)
VS
VD
CCPS
4000
C
R_{cr}
L_s
R_s
(b)
I, kA
7
6
5
4
3
2
1
0
2.5
5
7.5
10
12.5
15
17.5
20
t, ms

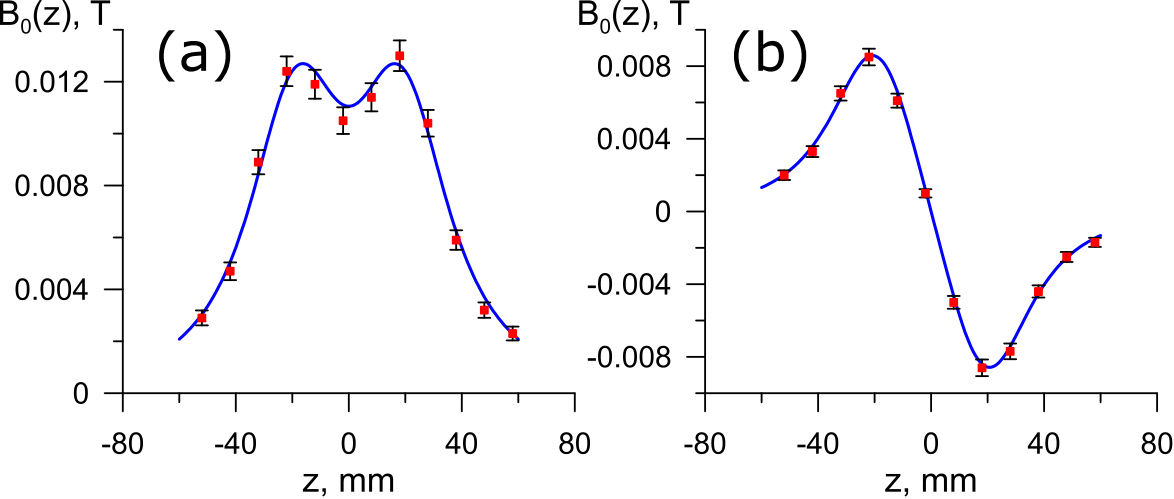
B0(z), T
(a)
0.012
0.008
0.004
0
-80
-40
0
40
80
z, mm
B0(z), T
(b)
0.008
0.004
0
-0.004
-0.008
-80
-40
0
40
80
z, mm

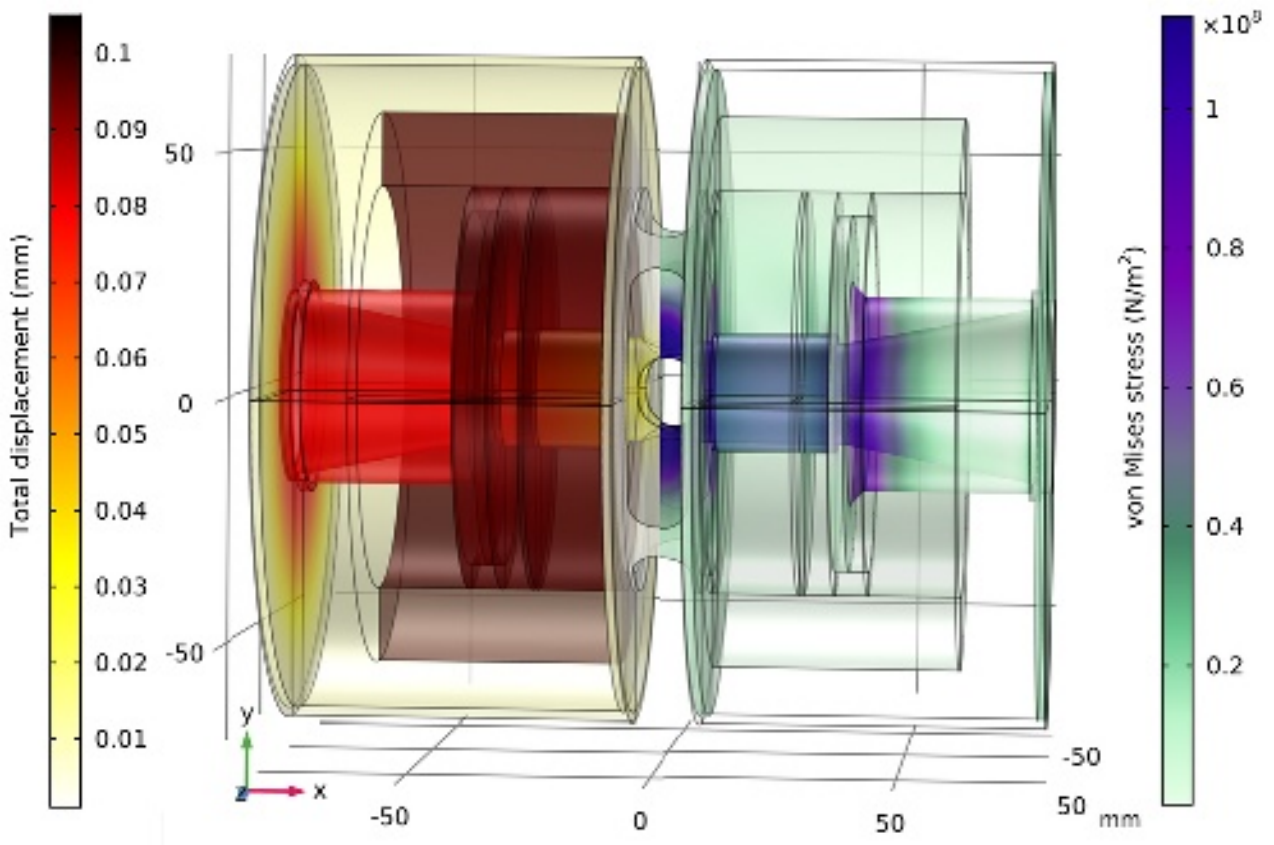
Total displacement (mm)
0.1
0.09
0.08
0.07
0.06
0.05
0.04
0.03
0.02
0.01
von Mises stress (N/m²)
×10⁹
1
0.8
0.6
0.4
0.2
50
0
-50
y
x
z
-50
0
50
-50
50
mm

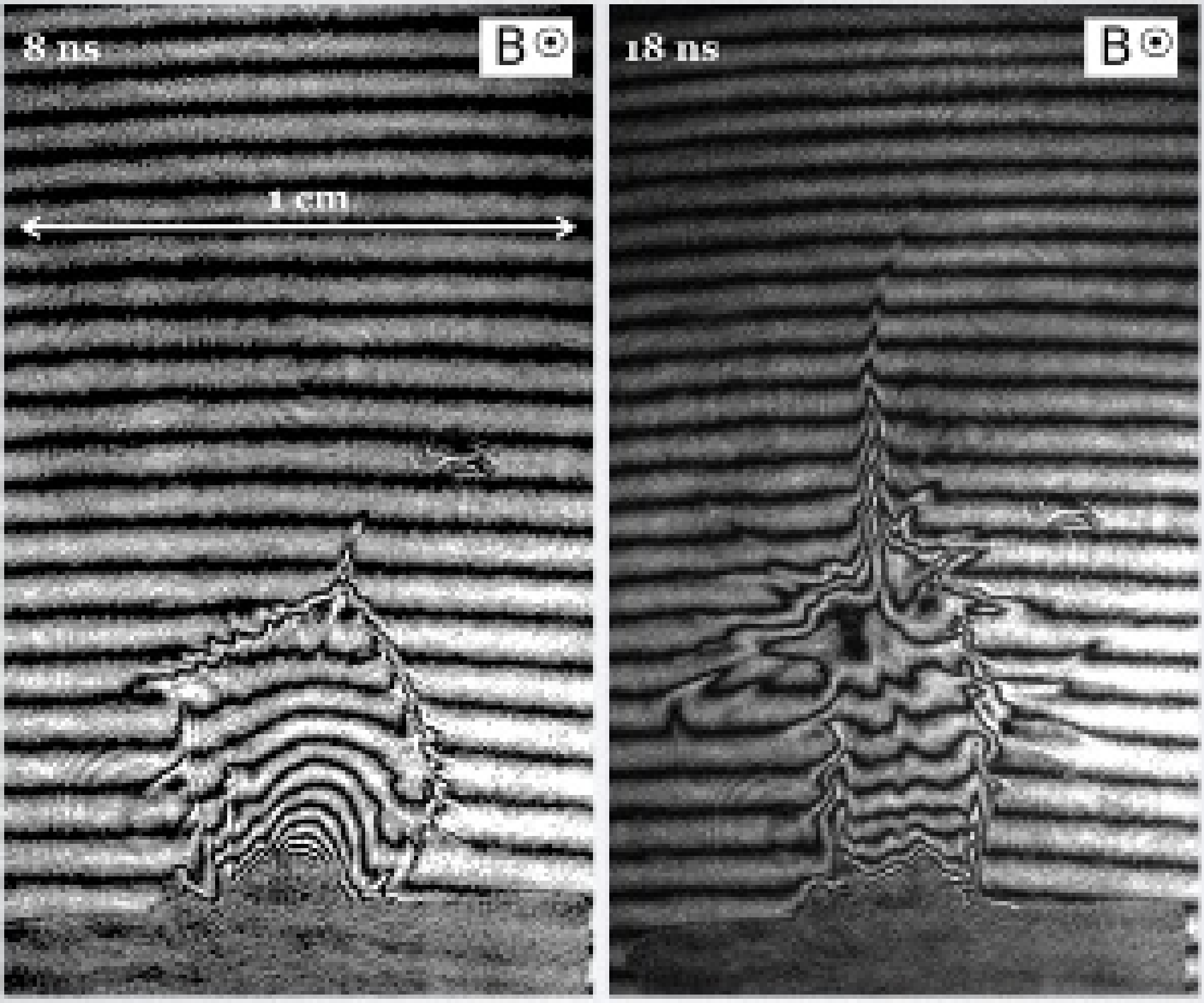
8 ns
B
1 cm
18 ns
B